Acta Crystallographica Section F
Structural Biology and Crystallization Communications
ISSN 1744-3091

Crystallization and preliminary X-ray crystallographic analysis of the hexameric human p97/VCP ND1 fragment in complex with the UBX domain of human FAF1

Wonchull Kang and Jin Kuk Yang*

Department of Chemistry, College of Natural Sciences, Soongsil University, Seoul 156-743, Republic of Korea

Correspondence e-mail: jinkukyang@ssu.ac.kr

Received 11 April 2011
Accepted 5 August 2011

The UBX domain of Fas-associated factor 1 (FAF1) binds to the N domain of p97/VCP, a multi-functional hexameric ATPase, and FAF1 thus inhibits the proteasome-mediated protein-degradation process assisted by p97/VCP. Here, crystallization of the hexameric p97/VCP ND1 fragment in complex with the FAF1 UBX domain is reported. Wild-type p97/VCP ND1 in complex with FAF1 UBX crystallized into very thin sheet-shaped crystals which turned out to be of poor diffraction quality. Therefore, in order to acquire a better diffraction-quality crystal, three mutants of p97/VCP ND1 were generated based on the surface-entropy reduction method. Of these, a triple mutant was the most successful in producing diffraction-quality crystals suitable for subsequent structural analysis. X-ray data were collected to 3.60 Å resolution and the crystals belonged to space group *I*222, with unit-cell parameters a = 166.28, b = 170.04, c = 255.99 Å. The Matthews coefficient and solvent content were estimated to be 5.78 Å^3 Da^{-1} and 78.72%, respectively.

1. Introduction

AAA+ family ATPases are classified into two subgroups, type I and type II, on the basis of the number of ATPase domains that they include. The type II proteins contain two ATPase domains, referred to as the D1 and D2 domains, and the type I proteins contain only one ATPase domain, termed D2. In addition to the ATPase domains, less conserved domains are often found at the N-terminus (N domain) or the C-terminus and are implicated in adaptor binding (Dougan *et al.*, 2002). p97/VCP (valosin-containing protein) is a multi-functional type II ATPase of the AAA+ family containing an N domain, a D1 domain and a D2 domain. Structural studies to date have revealed that p97/VCP forms a homohexamer of *P*6 point-group symmetry through its D1 and D2 domains; the N domain at the perimeter of the hexameric ring is responsible for binding to various adaptor proteins, through which p97/VCP can become involved in diverse cellular processes (Zhang *et al.*, 2000; DeLaBarre & Brunger, 2003; Vij, 2008).

The UBX domain, comprising about 80 amino-acid residues, is a general p97/VCP-binding module found in an increasing number of proteins such as p47 and FAF1 (Fas-associated factor 1; Schuberth & Buchberger, 2008). The UBX domain has been shown to directly bind to the N domain of p97/VCP and structural details of the interaction were initially revealed from the crystal structure of a p97/VCP ND1 fragment in complex with p47 UBX at 2.9 Å resolution (Dreveny *et al.*, 2004). In this crystal structure, only two of the six N domains of the hexameric p97/VCP ND1 are occupied by p47 UBX domain molecules to form a 6:2 complex, even though isothermal titration calorimetry experiments indicated that p97/VCP ND1 can bind six p47 UBX domain molecules (Dreveny *et al.*, 2004). The discrepancy in the binding ratio was presumably caused by the crystal-packing process (Dreveny *et al.*, 2004). Interestingly, p97/VCP and full-length p47 have been shown to form a 6:3 complex (Kondo *et al.*, 1997; Beuron *et al.*, 2006).

Human FAF1, composed of 650 amino-acid residues, contains five domains: UBA at the N-terminus, two tandem UBLs, UAS and UBX at the C-terminus (Song *et al.*, 2005; Menges *et al.*, 2009). FAF1 was initially identified as an Fas-interacting protein, but has subsequently

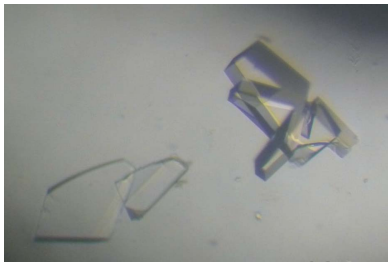

been revealed to also be involved in proteasome-mediated protein degradation. The two terminal domains of FAF1 are responsible for this function. The N-terminal UBA domain interacts with ubiquitins conjugated to the client proteins and the C-terminal UBX domain binds to the N domain of p97/VCP, which may serve as a molecular chaperone that presents the ubiquitinated client proteins to the proteasome. Through these two types of interactions, FAF1 inhibits the protein-degradation process and consequently enhances cell death (Song *et al.*, 2005). In an effort to elucidate the structural basis of the function of FAF1 in the p97/VCP-related proteasomal protein-degradation process, we initiated structural studies on the interaction between these two proteins. Here, we report the crystallization of the human p97/VCP ND1 fragment in complex with the human FAF1 UBX domain. A diffraction-quality crystal was obtained using a surface-entropy-reduced mutant of p97/VCP ND1. Sequence alignment between FAF1 and p47 identified 17 identical residues in the 78 residues in the UBX domain, giving 22% identity (*UniProt Align*; http://www.uniprot.org/align). Comparison of the structures of UBX domains from two different adaptor proteins, our current FAF1 and the previously reported p47 (Dreveny *et al.*, 2004), in complex with the hexameric p97/VCP ND1 will be valuable for establishing the common mechanism of the complex architecture.

2. Experimental procedures

2.1. Cloning and site-directed mutagenesis

The gene region for residues 21–458 of human p97/VCP including its N domain and D1 domain, the so-called ND1 fragment, was amplified by polymerase chain reaction from its cDNA (KRIBB, Republic of Korea; clone ID hMU007236). The amplified gene was digested with restriction enzymes *Bam*HI and *Eco*RI and ligated into a modified pET vector (a gift from Dr K. K. Kim of Sungkyunkwan University, Republic of Korea). The constructed expression vector is designed to produce the p97/VCP ND1 fragment, either wild type or mutant, in fusion with His-tagged thioredoxin which can be cleaved off by TEV protease. Therefore, the overproduced protein contains the following sequences from the N-terminus: (hexahistidine tag)–(thioredoxin)–(TEV recognition site, ENLYFQG)–(p97/VCP ND1 fragment, residues 21–458). After TEV cleavage, the extra sequence Gly-Ser which is translated from a *Bam*HI site remains attached to the N-terminal end of the p97/VCP ND1 fragment. Three mutants (K62A/K63A, E192A/D193A/E194A and E294A/K295A) were generated using the QuikChange Site-Directed Mutagenesis kit (Stratagene, USA). The nucleotide sequences for the wild type and the mutants were confirmed by sequencing (Bionics, Republic of Korea).

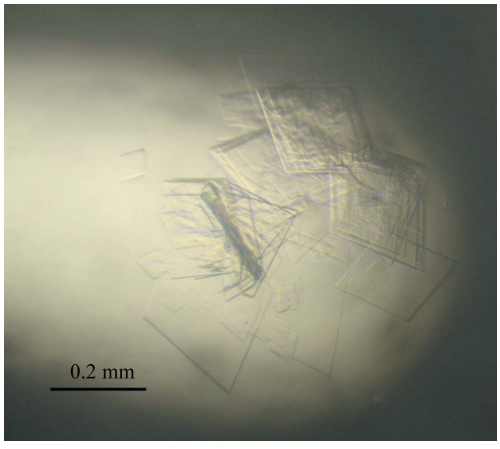

Figure 1
Crystals of the wild-type human p97/VCP ND1 fragment in complex with the FAF1 UBX domain.

2.2. Protein overproduction and purification

Escherichia coli strain Rosetta2 (DE3) was transformed with the expression vector and then cultured with shaking at 310 K in Luria–Bertani medium containing 30 µg ml^{-1} kanamycin. When the OD_{600} reached 0.6, the culture was cooled to 298 K and protein overproduction was induced by adding isopropyl β-D-1-thiogalactopyranoside (IPTG) to a final concentration of 0.5 m*M*. The cells were cultured at 298 K for an additional 16 h after IPTG induction and harvested by centrifugation at 5000 rev min^{-1} (4416*g*) for 30 min (Hanil Supra 22K with rotor 11, Republic of Korea).

The harvested cells were resuspended in working buffer [20 m*M* Tris–HCl, 5%(*v*/*v*) glycerol, 0.1 m*M* TCEP, 100 m*M* sodium chloride pH 8.0] containing 10 m*M* imidazole and 0.1 m*M* phenylmethylsulfonyl fluoride. The resuspended cells were lysed by sonication with a VCX500 ultrasonic processor (Sonics & Materials, USA) and the cell lysate was centrifuged at 15 000 rev min^{-1} for 60 min (Hanil Supra 22K with rotor 7, Republic of Korea). The supernatant was filtered through a membrane filter with 0.45 µm pore size (Advantec, Japan). The sample was then loaded onto a HisTrap column (GE Healthcare Bioscience, USA) and the bound protein was eluted with a 0–0.5 *M* imidazole gradient. The eluted sample was passed through a HiPrep Desalting column (GE Healthcare Bioscience, USA) to remove the imidazole and was then treated with TEV protease (van den Berg *et al.*, 2006) at a molar ratio of 1:100 at 293 K overnight. The sample was loaded onto a HisTrap column to separate the p97/VCP ND1 fragment from the cleaved fusion partner containing the His tag. Unbound flowthrough sample containing the p97/VCP ND1 fragment was collected and concentrated by centrifugal ultrafiltration (Amicon Ultra, Millipore, USA). Gel filtration was performed on a Superdex 200 column (GE Healthcare Bioscience, USA) pre-equilibrated with working buffer. The final purified p97/VCP ND1 fragment sample was concentrated to 1 m*M*. The human FAF1 UBX domain (residues 571–650) was cloned and overproduced as described previously (Shin *et al.*, 2010). Separately purified p97/VCP ND1 and FAF1 UBX samples were mixed in a 1:1 ratio for crystallization. The purity of the protein was judged by SDS–PAGE and its concentration was determined by measuring the absorbance at 280 nm, employing the calculated extinction coefficient of 0.50 mg^{-1} ml cm^{-1} (http://www.expasy.org).

2.3. Crystallization and X-ray data collection

Crystallization conditions were initially screened using commercial screening kits from Hampton Research, Emerald BioSystems and Qiagen. Crystals were grown by the hanging-drop vapour-diffusion method. 2 µl protein solution was mixed with an equal volume of reservoir solution and the mixture was equilibrated against 0.5 ml reservoir solution at 295 K. Refinement of the reservoir-solution composition was carried out by varying the concentration of the component chemicals. Crystals were soaked for 1–2 s in a 10 µl droplet of a cryoprotective solution, which had the composition of the well solution with an additional 10–20%(*v*/*v*) glycerol, and were then flash-cooled in liquid nitrogen before data collection.

X-ray diffraction data were collected at 100 K using an ADSC Quantum 315r CCD detector on synchrotron beamline 4A of Pohang Light Source, Republic of Korea. 300 images were collected for the full data set and each image was recorded with an exposure of 30 s

per 1° oscillation range. Intensity data were processed, merged and scaled with *MOSFLM* and *SCALA* from the *CCP*4 program suite (Powell, 1999; Winn *et al.*, 2011).

3. Results and discussion

The human p97/VCP ND1 fragment (residues 21–458) was overproduced in *E. coli* and purified by column chromatography. The FAF1 UBX domain was overproduced and purified as described previously (Shin *et al.*, 2010). The proteins were separately concentrated to 1.0 m*M* and mixed in a 1:1 ratio for crystallization trials. Very thin sheet-shaped crystals grew in 1–2 d from several reservoir-solution compositions containing ammonium sulfate as a precipitating agent; one representative composition was 1.3 *M* ammonium sulfate and 0.1 *M* MES pH 6.5 (Fig. 1). In order to check whether the crystals contained both p97/VCP ND1 and FAF1 UBX, the crystals were taken out of the drop, washed with reservoir solution to remove the protein solution on the crystal surface and subjected to SDS–PAGE. The results clearly indicated that the crystals contained

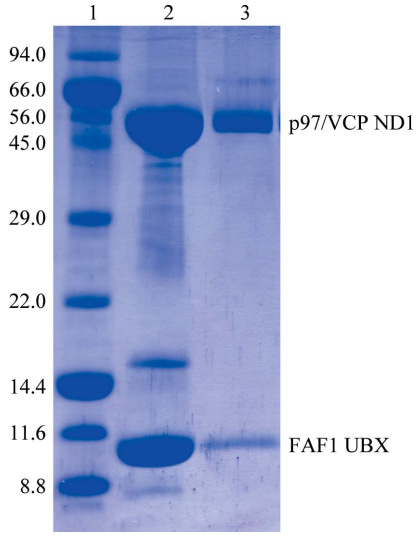

Figure 2
SDS–PAGE of the crystals. Lane 1 contains molecular-size markers; their molecular masses are given in kDa. Lane 2 contains protein sample and lane 3 contains crystals of the p97/VCP ND1 fragment and FAF1 UBX domain.

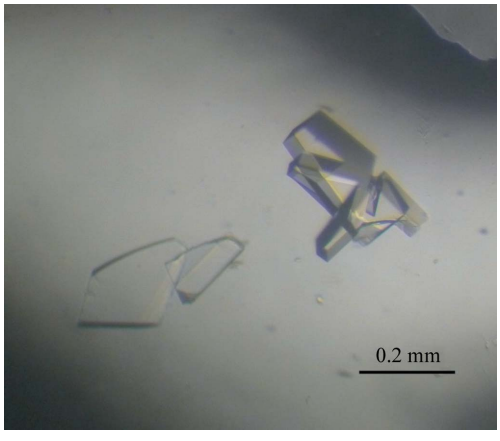

Figure 3
Crystals of the E192A/D193A/E194A mutant of human p97/VCP ND1 fragment in complex with the FAF1 UBX domain.

Table 1
Summary of data-collection statistics.

Values in parentheses are for the highest resolution shell.

Space group	*I*222
Unit-cell parameters (Å)	a = 166.28, b = 170.04, c = 255.99
Resolution (Å)	30.00–3.60 (3.79–3.60)
No. of measured reflections	483345
No. of unique reflections	42143
$R_{\rm merge}$† (%)	8.4 (35.7)
Completeness (%)	99.1 (97.1)
$\langle I/\sigma(I)\rangle$	8.1 (2.2)
Multiplicity	11.4 (11.4)

† $R_{\rm merge} = \sum_{hkl}\sum_i |I_i(hkl) - \langle I(hkl)\rangle| / \sum_{hkl}\sum_i I_i(hkl)$, where $I_i(hkl)$ is the intensity of reflection hkl, $\sum_{hkl}$ is the sum over all reflections and $\sum_i$ is the sum over i measurements of reflection hkl.

both proteins (Fig. 2). However, a diffraction experiment on beamline 4A of Pohang Light Source revealed that this sheet-shaped crystal had poor diffraction quality, with a diffraction limit lower than 5 Å and a highly anisotropic diffraction pattern. We concluded that these easily formed sheet-shaped crystals were not suitable for subsequent data collection and structural analysis. Therefore, we designed three different mutants (K62A/K63A, E192A/D193A/E194A and E294A/K295A) based on the surface-entropy reduction method (Cooper *et al.*, 2007); the mutation sites were selected to be on the surface distant from the UBX-binding interface identified in the previously reported crystal structure of the mouse p97/VCP ND1 fragment in complex with p47 UBX (Dreveny *et al.*, 2004). Three mutant protein samples were purified using the same procedure as for the wild type and concentrated to 1.0 m*M*. The purified mutant protein samples were subjected to screening of crystallization conditions in a mixture with FAF1 UBX in a 1:1 molar ratio. Of the three mutants, the triple mutant E192A/D193A/E194A crystallized most successfully; crystals of around 50 µm thickness (Fig. 3) grew from condition No. 79 of Qiagen Protein Complex Suite (3.0 *M* sodium formate and 0.1 *M* Tris pH 7.5).

The crystals diffracted to 3.60 Å resolution on beamline 4A at Pohang Light Source, Republic of Korea. The crystals belonged to the *I*-centred orthorhombic system, with unit-cell parameters a = 166.28, b = 170.04, c = 255.99 Å. The diffraction data set contained 42 143 unique reflections and was 99.1% complete, with a multiplicity of 11.4 and an $R_{\rm merge}$ of 8.4%. Table 1 summarizes the statistics of the data collection. The molecular masses of the p97/VCP ND1 mutant and FAF1 UBX are 48 937 and 9822 Da, respectively. Structure solution was attempted using molecular replacement with *Phaser* (McCoy *et al.*, 2007). The search models for the molecular replacement were taken from the previously reported crystal structures of murine p97/VCP ND1 (PDB entry 1s3s; Dreveny *et al.*, 2004) and human FAF1 UBX (PDB entry 3qca; Kang & Yang, 2011). Three molecules of p97/VCP ND1, *i.e.* half of its hexamer, and one molecule of FAF1 UBX were successfully located, as judged by the RFZ and TFZ scores of 3.5 and 6.2, respectively, and by the electron density in *Coot* (Emsley & Cowtan, 2004). Given that three p97/VCP ND1 and one FAF1 UBX are present in the asymmetric unit, the Matthews coefficient is 5.78 Å^3 Da^{-1} (Matthews, 1968) and the corresponding solvent content is 78.72%. Model rebuilding and structure refinement are under way.

This work was supported by a Korea Research Foundation Grant funded by the Korean Government (MOEHRD, Basic Research Promotion Fund; KRF-2008-331-C00177) and also by a grant from the Korea Healthcare Technology R&D Project, Ministry of Health

and Welfare, Republic of Korea (A092006). The authors thank the staff of Pohang Light Source beamline 4A.

References

Berg, S. van den, Löfdahl, P. A., Härd, T. & Berglund, H. (2006). *J. Biotechnol.* **121**, 291–298.
Beuron, F., Dreveny, I., Yuan, X., Pye, V. E., McKeown, C., Briggs, L. C., Cliff, M. J., Kaneko, Y., Wallis, R., Isaacson, R. L., Ladbury, J. E., Matthews, S. J., Kondo, H., Zhang, X. & Freemont, P. S. (2006). *EMBO J.* **25**, 1967–1976.
Cooper, D. R., Boczek, T., Grelewska, K., Pinkowska, M., Sikorska, M., Zawadzki, M. & Derewenda, Z. (2007). *Acta Cryst.* D**63**, 636–645.
DeLaBarre, B. & Brunger, A. T. (2003). *Nature Struct. Biol.* **10**, 856–863.
Dougan, D. A., Mogk, A., Zeth, K., Turgay, K. & Bukau, B. (2002). *FEBS Lett.* **529**, 6–10.
Dreveny, I., Kondo, H., Uchiyama, K., Shaw, A., Zhang, X. & Freemont, P. S. (2004). *EMBO J.* **23**, 1030–1039.
Emsley, P. & Cowtan, K. (2004). *Acta Cryst.* D**60**, 2126–2132.
Kang, W. & Yang, J. K. (2011). *Biochem. Biophys. Res. Commun.* **407**, 531–534.
Kondo, H., Rabouille, C., Newman, R., Levine, T. P., Pappin, D., Freemont, P. & Warren, G. (1997). *Nature (London)*, **388**, 75–78.
Matthews, B. W. (1968). *J. Mol. Biol.* **33**, 491–497.
McCoy, A. J., Grosse-Kunstleve, R. W., Adams, P. D., Winn, M. D., Storoni, L. C. & Read, R. J. (2007). *J. Appl. Cryst.* **40**, 658–674.
Menges, C. W., Altomare, D. A. & Testa, J. R. (2009). *Cell Cycle*, **8**, 2528–2534.
Powell, H. R. (1999). *Acta Cryst.* D**55**, 1690–1695.
Schuberth, C. & Buchberger, A. (2008). *Cell. Mol. Life Sci.* **65**, 2360–2371.
Shin, H. Y., Kang, W., Lee, S. Y. & Yang, J. K. (2010). *Acta Cryst.* F**66**, 41–43.
Song, E. J., Yim, S.-H., Kim, E., Kim, N.-S. & Lee, K.-J. (2005). *Mol. Cell. Biol.* **25**, 2511–2524.
Vij, N. (2008). *J. Cell. Mol. Med.* **12**, 2511–2518.
Winn, M. D. *et al.* (2011). *Acta Cryst.* D**67**, 235–242.
Zhang, X., Shaw, A., Bates, P. A., Newman, R. H., Gowen, B., Orlova, E., Gorman, M. A., Kondo, H., Dokurno, P., Lally, J., Leonard, G., Meyer, H., van Heel, M. & Freemont, P. S. (2000). *Mol. Cell*, **6**, 1473–1484.